doi.org/10.36721/PJPS/2026.40.16941.1

Comprehensive analysis of the therapeutic effect of lipid-coated hybrid nanoparticles for breast cancer therapy

Tehreem Arshad[1], Muhammad Ovais Omer[1*], Ali Sharif[2], Adeel Sattar[1], Arfan Ahmad[3], Imran Tariq[4] and Sajid Ali[5]

[1]Department of Pharmacology and Toxicology, Faculty of Biosciences, University of Veterinary and Animal Sciences, Lahore, 54000, Punjab, Pakistan

[2]Department of Pharmacology, Institute of Pharmacy, Faculty of Pharmaceutical and Allied Health Sciences, Lahore College for Women University, Lahore, 54000, Punjab, Pakistan

[3]Institute of Microbiology, University of Veterinary and Animal Sciences, Lahore, 54000, Punjab, Pakistan

[4]Punjab University College of Pharmacy, University of the Punjab, Lahore, 54000, Punjab, Pakistan

[5]Physical Chemistry, Department of Chemistry, Uppsala University, Uppsala, 75105, Sweden

Abstract: **Background**: Nanoparticles have gained considerable attention as versatile platforms for the diagnosis and treatment of different diseases, particularly cancer. Lipid-coated hybrid nanoparticles (LCHNPs), comprising a polymeric core enveloped by a lipid shell, offer improved targeting and potential solutions for multidrug-resistant cancers. **Objective**: To develop and preclinically evaluate a dual-drug LCHNP system co-delivering Tamoxifen and Gemifloxacin for enhanced breast cancer therapy. **Methods**: An experimental *in-vitro* and *in-vivo* study was conducted to develop and evaluate lipid-coated hybrid nanoparticles (LCHNPs) co-delivering Tamoxifen and Gemifloxacin using MCF-7 cells and a DMBA-induced mammary tumor model in female Albino Wistar rats.Poly(lactic-co-glycolic acid) (PLGA) nanoparticles loaded with Tamoxifen were prepared by the solvent evaporation method and liposomes loaded with Gemifloxacin were prepared by the thin-film hydration technique. The two systems were subsequently fused to generate LCHNPs. Physicochemical and structural characterization was carried out using dynamic light scattering (DLS), Fourier transform infrared spectroscopy (FTIR) and scanning electron microscopy (SEM). **Results**: The mean particle sizes of Tamoxifen nanoparticles, Gemifloxacin liposomes and LCHNPs were 175.3 ± 1.97 nm, 201.2 ± 2.45 nm and 215.7 ± 2.25 nm, with zeta potentials of +5.5 mV, −12.9 mV and +0.6 mV, respectively. Encapsulation efficiencies reached 96.41 ± 0.66% for nanoparticles and 91.22 ± 1.1% for liposomes. FTIR confirmed successful drug incorporation, while SEM imaging demonstrated smooth particle surfaces. LCHNPs exhibited the lowest IC_{50} value among the tested formulations (IC□□ = 3.83 µM). RT-qPCR (quantitative reverse transcription polymerase chain reaction) analysis demonstrated a significant upregulation of *CHEK2* (2.67 ± 1.66-fold) and downregulation of *BRCA1* (0.65 ± 0.19-fold) in the LCHNP-treated group compared with the disease control. *In-vivo* evaluation in a DMBA (dimethylbenz[*a*]anthracene)-induced mammary tumor model in female Albino Wistar rats (n = 6/group) confirmed the enhanced antitumor efficacy of LCHNPs, as evidenced by reduced tumor incidence and favorable biochemical, hematological and histopathological profiles. **Conclusion**: Lipid-coated hybrid nanoparticles exhibited enhanced anticancer activity. This study provides a preclinical evaluation of a dual-drug lipid-coated PLGA hybrid nanoparticle co-delivering Tamoxifen and Gemifloxacin, a formulation that has not been previously reported for breast cancer therapy.

Keywords: Breast cancer; Cytotoxicity; Gemifloxacin; Lipid-coated nanoparticles; Tamoxifen

Submitted 09-06-2026 – Revised 14-07-2026 – Accepted 01-08-2026

INTRODUCTION

The aberrant growth of epithelial cells in breast tissue causes breast cancer (Hoxha *et al.*, 2024). Breast cancer continues to pose a major global health challenge, being the most commonly diagnosed malignancy among women and one of the leading causes of cancer-related deaths. Each year, approximately 2.3 million women are diagnosed with the disease and nearly 670,000 deaths are attributed to breast cancer worldwide, underscoring its substantial public health impact (Bray *et al.*, 2024). Tamoxifen adjuvant treatment is recommended in pre and postmenopausal women with breast cancer (Agardan *et al.*, 2020). Tamoxifen (TAM) selectively modulates estrogen receptor (ER) activation by preventing estrogen from binding to its receptors in breast tissue, thereby suppressing estrogen-driven proliferation. Gemifloxacin belongs to the quinolone class and exhibits antibacterial function by inhibiting Topoisomerase II and IV (Firuzabadi and Asadi, 2021). It has been reported that by interfering with the S and G2/M Phases of the cell cycle, fluoroquinolones reduce DNA synthesis and tumor progression (Kassab *et al.*, 2024). These properties position Gemifloxacin as a promising adjunct agent capable of inducing replication stress and potentiating apoptosis in cancer cells. Preclinical investigations have shown that Gemifloxacin can reduce the proliferation of breast cancer cells and inhibit the

*Corresponding author: e-mail: drovaisomer@uvas.edu.pk

Article in Press

epithelial-to-mesenchymal transition (EMT), reduce cancer stem cell properties and impair cellular migration through modulation of multiple signaling pathways, including NF-κB and Snail, which are associated with tumor progression and metastasis (da Silva *et al.*, 2026).

Unlike Tamoxifen, which primarily targets estrogen receptor signaling, Gemifloxacin appears to influence pathways involved in tumor invasion and metastatic behavior. These complementary mechanisms provided the scientific rationale for investigating the co-delivery of Tamoxifen and Gemifloxacin within a lipid-coated hybrid nanoparticle system. Nevertheless, these findings remain largely confined to experimental models and clinical evidence supporting the use of Gemifloxacin as an anticancer agent is still limited. The formulation strategy in this study was based on the hypothesis that simultaneous inhibition of hormonal signaling and induction of DNA damage may increase the susceptibility of breast cancer cells to treatment. This concept served as the scientific rationale for developing the formulation; however, it was not experimentally validated in the present work through functional assays assessing DNA damage or apoptosis. Gemifloxacin in combination with Tamoxifen was intended to investigate the simultaneous modulation of endocrine signaling and additional tumor-promoting pathways. It could improve therapeutic outcomes within a lipid-coated hybrid nanoparticle delivery system. Nevertheless, the anticancer potential of Gemifloxacin remains largely preclinical and further mechanistic and clinical studies are required to establish its therapeutic role.

Gemifloxacin was chosen instead of widely validated anticancer drugs such as docetaxel or doxorubicin because its clinical approval, well-characterized safety profile and favorable pharmacokinetic properties make it an attractive candidate for drug repurposing. Moreover, its proposed topoisomerase-mediated mechanism is expected to complement Tamoxifen without substantially increasing overlapping toxicities. Accordingly, Gemifloxacin was investigated as a rational exploratory partner for combination therapy rather than as an alternative to conventional cytotoxic agents.

Chemotherapy causes severe adverse effects in patients because of the non-selective therapeutic actions of drugs on normal cells as well as diseased cells. Over the past few decades, to increase the effectiveness and efficacy of chemotherapeutic drugs, a novel drug delivery system has been developed in which nanoparticles encapsulating therapeutic agents are used (Mangu *et al.*, 2026). Nanoparticles have emerged as promising carriers to enable targeted delivery to tumors or damaged organs (Wang *et al.*, 2022; Zhang *et al.*, 2020). Nanocarriers can enhance the therapeutic index of existing drugs by reducing their toxicity, improving efficacy and maintaining a steady-state therapeutic concentration over an extended duration (Chatterjee and Kumar, 2022). Recent studies continue to expand the PLGA nanoparticle platform for breast cancer drug delivery and broader oncology applications (Kesharwani *et al.*, 2025; Ma *et al.*, 2025).

Previous studies reported enhanced anticancer activity by combining Tamoxifen with nanocarriers. Silver nanoparticle–Tamoxifen formulations produced synergistic cytotoxic effects with minimal genotoxicity in MCF-7 and MDA-MB-231 breast cancer cell (Rivera *et al.*, 2024). Similarly, lipid-coated mesoporous silica nanoparticles co-loaded with Tamoxifen and docetaxel have been developed to improve therapeutic efficacy and overcome CYP3A4-associated drug resistance in triple-negative breast cancer (Wang *et al.*, 2024). More recently, αvβ3 integrin aptamer-functionalized lipid-polymer hybrid nanoparticles co-delivering paclitaxel and Tamoxifen have demonstrated enhanced tumor-selective cytotoxicity in triple-negative breast cancer models (Narwade *et al.*, 2025). Previous combination strategies have largely involved conventional cytotoxic drugs or metal-based nanocarriers, both of which are associated with systemic toxicity and undesirable off-target effects.

In contrast, no published study has combined Tamoxifen with a repurposed non-oncologic agent that targets DNA damage and anti-migratory pathways through mechanisms distinct from those of standard chemotherapy. Addressing this unmet area provided the rationale for developing the present LCHNP formulation. The synergistic effects of lipid-based nanocarriers have been shown to enhance the efficacy and precision of polymeric nanoparticles (Alawi *et al.*, 2025). Although PLGA nanoparticles, lipid-coated hybrid nanocarriers and Tamoxifen-loaded nanoparticle formulations have been extensively investigated, there are currently no reports describing the co-delivery of Tamoxifen and Gemifloxacin within a single lipid-coated PLGA hybrid nanoparticle for breast cancer therapy. The present study addresses this gap by developing a dual-drug hybrid nanocarrier and evaluating its physicochemical properties, sustained drug release, anticancer efficacy and preliminary molecular effects in an experimental breast cancer model. Rather than establishing Gemifloxacin as a clinically validated anticancer agent, this work explores its potential as a repurposed therapeutic candidate within an advanced nanocarrier system.

MATERIALS AND METHODS

Chemicals and reagents

Tamoxifen citrate and Gemifloxacin mesylate were obtained as gift samples from Pharmedic Laboratories (Lahore,Pakistan).1,2-dipalmitoyl-sn-glycero-3-phosphatidylcholine (DPPC); 1,2-dipalmitoyl-sn-glycero-3-phosphoethanolamine-N-[methoxy(polyethylene glycol)-5000] (DPPE-mPEG$_{5000}$) and 2-dipalmitoyl-sn-glycero-3-phospho-(1′-rac-glycerol) (sodium salt) (DPPG)

Article in Press

were obtained as gift sample from Lipoid GmbH (Ludwigshafen, Germany). PLGA (Resomer® RG 503 H, Poly (D, L-lactide-co-glycolide)) was supplied by Evonik (Essen, Germany). Poly (vinyl alcohol) (PVA, Mowiol 4–88) was purchased from Kuraray (Hattersheim, Germany). Polysorbate 80 (Tween 80) and 3-(4,5-dimethylthiazol-2yl)-2,5-diphenyltetrazolium bromide (MTT) were obtained from Sigma Aldrich Chemie GmbH (Taufkirchen, Germany).Dimethyl sulfoxide (DMSO) was procured from Carl Roth GmbH & Co. (Karlsruhe, Germany).Chitosan [molecular weight 1526.464 g/mol] was purchased from MP Biomedicals LLC, Irvine, CA, USA.HPLC grade Organic solvents (chloroform ($CHCl_3$), methanol (MeOH) and Ethyl acetate) were obtained from VWR International (Darmstadt, Germany).Glacial acetic acid (≥99.8%; Merck, Germany; Cat. No. 100063), ethanol (lab grade, 96%; Merck; Cat. No. 100983) and formaldehyde solution (37%; Merck; Cat. No. 104003). TRIzol™ Reagent (Thermo Fisher Scientific, USA; Cat. No. 15596026), cDNA was synthesized with the RevertAid First Strand cDNA Synthesis Kit (Thermo Scientific; Cat. No. K1622) and quantitative PCR was performed using PowerUp™ SYBR™ Green Master Mix (Thermo Fisher Scientific; Cat. No. A25742).Sterile filtered ultra-pure (PureLab flex-4 dispenser, ELGA Lab water, High Wycombe, UK) water was used for all the experiments. All reagents were used as received unless otherwise specified. Phosphate-buffered saline (PBS) was freshly prepared, sterilized by filtration and stored at 4°C until use.

Preparation of tamoxifen-loaded PLGA nanoparticles

Tamoxifen nanoparticles were prepared by using the emulsion solvent evaporation method. Tamoxifen and PLGA were used at a drug-to-polymer ratio of 1:50 (w/w) (2 mg drug:100 mg PLGA). This ratio was selected based on previous reports demonstrating that low drug-to-polymer ratios improve encapsulation efficiency, maintain a narrow particle size distribution and reduce drug crystallization within PLGA nanoparticles. A stock solution of Tamoxifen (1mg/mL) was prepared in ethyl acetate. Then, PLGA (100 mg) was dissolved in a 5 mL ethyl acetate solution containing 2mg Tamoxifen. Subsequently, the solution was filtered through a 0.2-µm membrane filter, then introduced drop by drop into the 1% (w/v) polyvinyl alcohol (PVA) solution. The oil-in-water (o/w) emulsion was mixed using an Ultra-Turrax homogenizer at 15,000 rpm for 10 min, after which 1 ml (0.10%) chitosan and 14 ml ultrapure water were added dropwise using a syringe. Ethyl acetate (organic phase) was evaporated by continuous stirring (500 rpm) overnight at room temperature. Blank nanoparticles were prepared in the same way except for the addition of Tamoxifen. Then, nanoparticles were washed twice at 16,000 × g for 20 min and freeze-dried with 0.2% w/v PVA solution. The lyophilized nanoparticles were stored under refrigerated conditions (2-8°C) until further characterization and analysis (Ali *et al.*, 2021).

Preparation of gemifloxacin liposomes

The thin-film hydration technique was employed to fabricate Gemifloxacin-loaded liposomes. The lipids comprising DPPC, DPPG and DPPE-mPEG5000 (85:10:5) were dissolved in a chloroform/methanol (2:1) mixture. 2 mg Gemifloxacin was added to a lipid mixture to form drug-loaded liposomes. The organic solvents were vacuum-dried at 45 °C using a rotary evaporator. Subsequently, 1 mL of phosphate-buffered saline (PBS, pH 7.4) was used in the film hydration technique with continuous mixing to produce liposomes. To transform these multilamellar liposomes into unilamellar ones, they were sonicated for approximately 40 minutes in a bath-type sonicator. The liposomes produced were kept cold for further examination (Nandi *et al.*, 2021; Pandey *et al.*, 2025).

Preparation of lipid-enveloped nanoparticles

To fabricate lipid-coated hybrid nanoparticles (LCHNPs), different liposome-to-nanoparticle mass ratios were initially evaluated and an optimized liposome:PLGA nanoparticle ratio of 1:100 (w/w) was selected based on particle stability and physicochemical characteristics. The fusion process was used to produce the lipid layer on the particle surface. This ratio yielded stable hybrid nanoparticles with a uniform particle-size distribution and satisfactory colloidal stability. In summary, a suitable number of liposomes loaded with Gemifloxacin were introduced into the suspension of PLGA nanoparticles loaded with Tamoxifen and the mixture was then properly mixed. After 20 minutes of sonication and an hour of room-temperature incubation, the mixture induced spontaneous fusion of a self-organized lipid bilayer on the nanoparticles' surface (Ali *et al.*, 2021) (Jacob *et al.*, 2025). The formulation was independently prepared in triplicate (n = 3) following the same experimental procedure to evaluate batch-to-batch reproducibility. Physicochemical characterization was performed for each batch and the results are presented as mean ± SD, indicating consistent preparation of the lipid-coated hybrid nanoparticles. Batch-to-batch reproducibility was assessed by comparing particle size, polydispersity index (PDI) and zeta potential among the three independently prepared batches. No statistically significant differences ($p > 0.05$) were observed, indicating good reproducibility of the formulation process.

Encapsulation efficiency and loading capacity

Encapsulation efficiency was determined indirectly by quantifying the amount of free (unencapsulated) drug present in the supernatant. To do this, a supernatant containing free or unbound drug was obtained and a UV spectrophotometer was used to quantify the amount of encapsulated drug. To determine the Drug loading, supernatants of both formulations, nanoparticles and liposomes, were taken in a cuvette and the absorbance of both supernatants was measured using a UV spectrophotometer, Shimadzu model UV-1280, at 276 nm

Article in Press

and 264 nm, respectively and the absorbance was recorded and the encapsulation efficiency was calculated as (Uniyal *et al.*, 2026).

$$\%EE=\frac{\text{Amount of capsulated drug}}{\text{Total amount of drug added}}\times 100 \text{ ..... (1)}$$

$$\%LC=\frac{\text{Amount of drug capsulated}}{\text{Dry weight of nanoparticles}}\times 100 \text{ ..... (2)}$$

Evaluation of in-vitro drug release

PBS (pH 7.4) with 1% Tween 80 (v/v) was used to determine the release patterns of Gemifloxacin and Tamoxifen. Freshly prepared nanoparticles and liposomes were collected by centrifugation. The 0.5 mg Tamoxifen pellet was resuspended in 5 mL phosphate buffer mixture Then nanoparticles were placed in an incubator at 37 °C and 100 rpm. During this study, 0.5 mL of the sample was taken at specified time intervals. Supernatant was separated after centrifugation of the sample at 15,000 × g for 10 min. To confirm sink conditions for the pellet sample, the pellet was resuspended in a Phosphate buffer solution (PBS; pH 7.4) containing 1% (v/v) Tween 80 and the original nanoparticle suspension was then prepared. The US/VIS spectrophotometer at 276 nm was used to determine the Tamoxifen concentrations. The remaining drug amount in the nanoparticles could be determined by dissolving a nanoparticle pellet in acetonitrile. Blank (no drug) PLGA nanoparticles for all subtraction measurements were processed in the same way (Ali, 2019; Anand *et al.*, 2021). *In-vitro* release of Gemifloxacin from liposomes was conducted by dialysis in a dialysis membrane with 200 ml of PBS (pH 7.4).Briefly, 1 mL of the formulation was transferred into a dialysis bag and immersed in 200 mL of phosphate-buffered saline (PBS) contained in a 250 mL conical flask. The flask was placed on a magnetic stirrer and the release medium was maintained at 37°C with continuous stirring at 250 rpm. At predetermined time intervals, 0.5 mL of the release medium was withdrawn using a micropipette and replaced with an equal volume of fresh PBS to maintain a constant volume. The collected samples were analyzed spectrophotometrically at 264 nm and the drug concentration was determined using a previously established standard calibration curve.

Physicochemical characterization of nanoparticles, liposomes and lipid-coated nanoparticles

Several techniques were used to analyze the prepared nanoparticles, liposomes and lipid-coated nanoparticles, including FTIR, scanning electron microscopy, zeta potential measurements and a particle size analyzer.

Ultraviolet–visible spectrophotometry

Drug incorporation into the Tamoxifen-loaded PLGA nanoparticles was assessed using UV–visible spectrophotometry. After centrifugation, the supernatant containing any unencapsulated Tamoxifen was collected and its absorbance spectrum was recorded between 200 and 400 nm. Blank PLGA nanoparticles served as the reference. Comparison of the absorption profiles enabled indirect confirmation of Tamoxifen encapsulation and facilitated quantification of the free drug remaining in the dispersion (Sahin *et al.*, 2025).

Particle size and zeta potential

It is used to measure the effective electric charge on the surface of nanoparticles. Zeta sizer measures the zeta potential of drug-loaded nanoparticles. Gemifloxacin and Tamoxifen nanoparticle samples were diluted with water (0.1 mL) and transferred into the electrophoretic cell, where an electric field strength of 15.2 V/cm was applied. The final lipid-coated hybrid nanoparticle (LCHNP) suspension was adjusted to 1 mg/mL before physicochemical characterization and biological evaluation. This concentration is within the range commonly used for PLGA-based nanoparticle formulations, providing sufficient colloidal stability while minimizing multiple scattering during particle-size analysis (Maretti *et al.*, 2025).

Scanning electron microscopy (SEM)

SEM was used to characterize the nanoparticles. It provides the morphological and elemental distribution of the sample at the Nano level (Sharmin and Bhuiyan, 2019). Tamoxifen nanoparticles were irradiated with UV light under laminar flow to ensure cleanliness. The sterilized nanoparticles were cautiously prepared in adhesive tape and then mounted on SEM stubs. The nanoparticle sample was placed in the SEM sample chamber and different scanning magnifications between ×15,000 and ×35,000 at a voltage of 20-30 kV were applied for investigation (Zhang *et al.*, 2025).

Fourier transform infrared spectroscopy (FTIR) analysis

The functional groups present in the sample material were identified by FTIR spectroscopy. Identification of Gemifloxacin and Tamoxifen nanoparticles was carried out using FTIR. The FTIR spectrometer was operated over the wavenumber range of 4000- 400 cm−1 (Aziz *et al.*, 2020). The stability of the nanoparticles was assessed by recording their FTIR spectra using an FTIR spectrophotometer (Mulè *et al.*, 2025). However, FTIR alone cannot unequivocally verify drug encapsulation or determine the precise localization of the drug within the hybrid nanostructure. Therefore, the FTIR findings should be interpreted as supportive evidence of successful formulation rather than definitive confirmation of encapsulation.

Stability study

The lyophilized nanoparticles were preserved in airtight amber glass vials using 5% (w/v) trehalose as a cryoprotective agent to minimize structural alterations during storage. Stability studies were conducted under two storage conditions: refrigerated temperature (4 ± 2°C) and controlled room temperature (25 ± 2 °C at 60 ± 5% relative

Article in Press

humidity). Samples were evaluated immediately after lyophilization (day 0) and after 30, 60 and 90 days of storage. At each predetermined interval, the formulations were characterized for particle size by dynamic light scattering, polydispersity index (PDI) and zeta potential.. Formulations were considered stable when no statistically significant differences ($p > 0.05$) were detected in these physicochemical properties relative to the freshly prepared nanoparticles, in accordance with established practices for the stability assessment of polymeric nanoparticle formulations (Gatto and Najahi-Missaoui, 2023).

Cell viability analysis (MTT assay)

The ability of the test compound to kill cells was assessed *in-vitro* using the MTT assay in the Vero (non-cancerous) and MCF-7 (cancerous) cell lines. The cytotoxic activity of the developed formulations was evaluated using the MTT colorimetric assay, which is based on the ability of metabolically active cells to reduce the yellow tetrazolium salt (MTT) to insoluble purple formazan crystals via mitochondrial oxidoreductases. MCF-7 cells were seeded into 96-well plates and allowed to attach for 24 h at 37°C in a humidified incubator containing 5% CO□.

The test formulations, including free Tamoxifen, Tamoxifen-loaded PLGA nanoparticles, free Gemifloxacin, Gemifloxacin-loaded liposomes and lipid-coated hybrid nanoparticles (LCHNPs), were serially diluted in Dulbecco's Modified Eagle Medium (DMEM) to obtain concentrations ranging from 0.78 to 200 µg/mL. After removing the culture medium, 100 µL of each formulation was added to the respective wells and the cells were incubated for an additional 24 h.

Following treatment, 100 µL of 0.25% (w/v) MTT solution was added to each well and the plates were incubated for 4 h to allow intracellular formazan formation. The MTT-containing medium was then carefully removed and 100 µL of 10% DMSO was added to dissolve the formazan crystals. Absorbance was recorded at 570 nm using a microplate reader. Cell viability was expressed as a percentage relative to untreated control cells. Each concentration was evaluated in three technical replicates and the entire experiment was performed independently three times (n = 3). Cell viability was computed relative to the control wells after absorbance at 570 nm was measured (Al-otaibi, 2021).

$$\% \text{ Inhibition} = \left(1 - \frac{ODt - ODb}{ODc - ODb}\right) \times 100 \quad \text{..... (3)}$$

Here, the average optical densities are represented by OD_t (test), OD_c (control) and OD_b (blank).

IC_{50} and selectivity index:

Dose–response curves were constructed using GraphPad Prism (version 8.0) and the half-maximal inhibitory concentration (IC_{50}) values were calculated by fitting the data to a nonlinear regression model of log(inhibitor) versus normalized response with a variable slope. Results are presented as mean ± SD. The concentrations required to induce 50% apoptosis (i.e., IC□□)) were appropriate and the Selective Index (S.I) was calculated.

$$S.I = \frac{IC50 \text{ of the drug in a normal cell line}}{IC50 \text{ of the drug in the cancer cell line}} \quad \text{..... (4)}$$

Gene expression analysis by RT-qPCR

The reaction mixtures for both genes were prepared using the SYBR Green system from Thermo Fisher Scientific. The amplification results were monitored in real time, with peaks and amplification curves displayed on the computer interface. The IC_{50} concentrations of Tamoxifen nanoparticles (6.27 µg/ml), Gemifloxacin liposomes (15.06 µg/ml) and lipid-coated hybrid nanoparticles (3.83 µg/ml) were applied to MCF-7 cells and left for 24 hours. Total RNA was extracted using TRIzol reagent. Cell viability following the treatment period was assessed using the trypan blue dye exclusion assay (Salimi *et al.*, 2025).

Extraction of RNA and formation of cDNA

The MCF-7 cell line was used to assess the expression of *BRCA1* and *CHEK2* genes after drug treatment. The four groups are categorized by treatment as: Tamoxifen nanoparticles, Gemifloxacin liposomes, Tamoxifen + Gemifloxacin co-loaded nanoparticles and a untreated control group. Each group has 3 samples; a total of 12 MCF-7 cell line samples were used for RNA extraction using the Trizol method.

In a sterile tube, cells were mixed with chloroform and Trizol, then centrifuged to obtain an RNA-containing layer. RNA precipitation was achieved by transferring this layer to another tube, followed by a 15-minute incubation in isopropanol. Then, it was washed with 75% ethanol and transferred to an isolated RNA pellet; the second centrifugation was done. The pellet was dried, resuspended in DEPC-treated water to eliminate RNase and stored between 4 ºC to -20 ºC for use. cDNA was formed by Thermo-Fisher Scientific cDNA synthesis kit. The proposed methodology produced the PCR master mix. By placing the PCR tube in a thermocycler, the optimal conditions were *achieved* to facilitate amplification. The produced cDNA was preserved at 4 ºC to -20 ºC until future use (Jeromin *et al.*, 2019).

Real-time PCR amplification

Gene expression analysis was performed using RT-PCR to quantify transcript copy numbers of the target genes (*CHEK2* and *BRCA1*). GAPDH served as the internal housekeeping gene for normalization of target gene expression. The PCR master mix was prepared according to the manufacturer's protocol and reactions were carried out under optimized conditions. Changes in gene expression were determined using the $2^{-\Delta\Delta CT}$ method, representing the fold change relative to the control group of untreated cells (Derismahafi *et al.*, 2025). Primer sequences are given below (Table 1).

Article in Press

Table 1: Primer sequences of the *CHEK2* and *BRCA1* genes (both Forward and Reverse).

Sr. No	Primers	Primer sequence	Length	Tm
1.	*CHEK2* Forward primer	5′-TCAGCAAGAGAGGCAGACCC-3′	20	54
2.	*CHEK2* Reverse primer	5′-ACAGCTCTCCCCCTTCCATC-3′	20	56
3.	*BRCA1* Forward primer	5′-GCCAAGGCAAGATAGAGG-3′	18	61
4.	*BRCA1* Reverse primer	5′-GTTGCCAACACGAGCTGA-3′	18	63

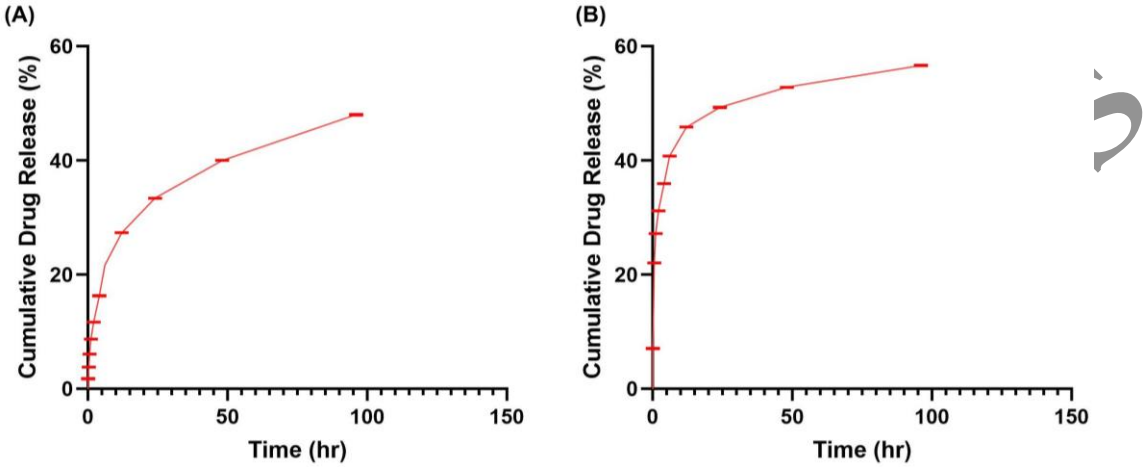


Fig. 1: Cumulative drug release of (A) Tamoxifen nanoparticles; (B) Gemifloxacin liposomes. Data are presented as mean ± SEM, with error bars representing the standard error of the mean.

In-vivo DMBA-induced mammary tumor

The rats were obtained from University of Veterinary and Animal Sciences. The animals were clinically healthy and were not genetically modified. No previous experimental procedures had been performed before commencement of the present study.A total of five groups (with each group containing n=6) of thirty female Albino Wistar rats (approx. 8-10 weeks with weight 180–220 g) were kept at a temperature of 23 ± 2 °C, with a humidity of 60 ± 10% and under a 12 h light and dark cycle. The rats in the experiment were provided with water and a standard pellet diet. Before dosing, the rats were allowed to acclimatize for 1 week.The individual rat was considered the experimental unit for the *in-vivo* analyses.

Inclusion criteria

Healthy female rats of the specified experimental age and body weight (approx. 8-10 weeks with weight 180–220 g) with no apparent signs of illness or abnormality, were included in the study.

Exclusion criteria

Animals showing signs of illness, abnormal behavior, significant health abnormalities, or conditions that could interfere with the experimental outcomes were excluded from the study.

The inclusion and exclusion criteria were established before commencement of the experiment. No animals, experimental units, or data points were excluded from the final analysis. A study protocol was prepared before commencement of the experiment but was not prospectively registered. The selected doses and administration schedules were based on previously published experimental studies and preliminary formulation considerations. The rats randomly assigned to Group I (n = 6) were considered the Negative control group and received no additional treatment; they received normal saline and standard food. Group II was designated as the positive control group, which received DMBA at 40 mg/kg/week via the intraperitoneal route for the period of 12 weeks. Group III received free Tamoxifen at 3 mg/kg orally daily, Group IV received free Gemifloxacin at 20 mg/kg orally daily and Group V received lipid-coated hybrid nanoparticles at 4 mg/kg twice in a week (Adefisan-Adeoye *et al.*, 2025). No single primary outcome measure was prespecified for sample-size determination. A group size of six rats was adopted based on established DMBA-induced mammary tumour studies, where similar sample sizes have been sufficient to detect significant differences in tumour development and biochemical outcomes among treatment groups. However, no a priori power/sample-size calculation is reported. Potential confounders related to treatment order, measurement order and cage location were not specifically controlled. To minimise assessment bias, all outcome measurements were performed by an investigator blinded to treatment allocation. The personnel responsible for animal allocation and treatment administration were aware of group assignments. Samples were coded before evaluation and group identities were revealed only after all outcome measurements had been completed. No formal humane endpoints were established; however, animals were monitored for signs of pain or distress throughout the experimental period.

Article in Press

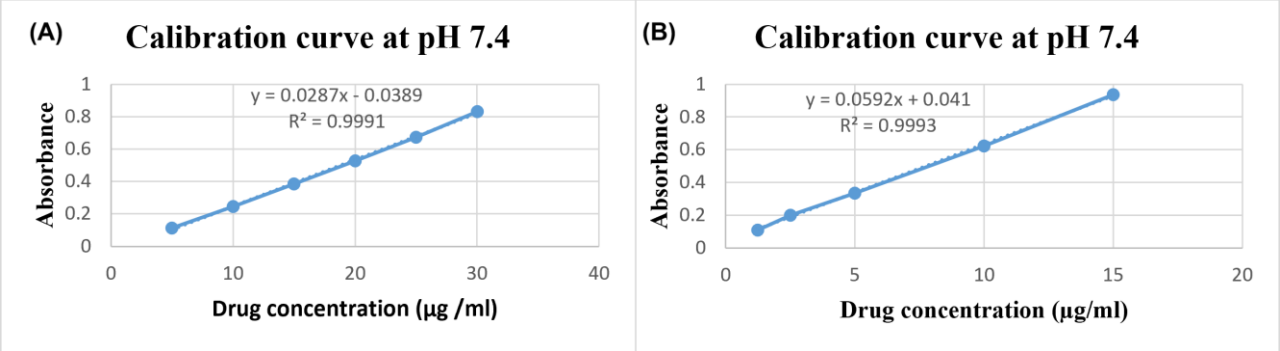


Fig. 2: Calibration curve of tamoxifen and gemifloxacin at 7.4 pH of (A) Tamoxifen nanoparticles, (B) Gemifloxacin liposomes.

Table 2: Diameter values are expressed as Mean ± S.D for 3 independent measurements (n=3).

Formulations	Diameter (nm) ± SD	PDI ± SD	ζ Potential (mV) ± SD
Tamoxifen nanoparticles	175.3 ± 1.97	0.03 ± 0.02	5.5 ± 1.11
Gemifloxacin liposomes	201.2 ± 2.45	0.25 ± 0.02	-12.9 ± 1.51
Lipid-coated hybrid NPs	215.7 ± 2.25	0.07 ± 0.03	0.6 ± 0.10

Biochemical, hematological analysis and histopathological studies

In the case of biochemical analysis, the parameters considered were total bilirubin, alkaline phosphatase (ALP), aspartate transaminase (AST) activity, alanine transaminase (ALT) activity, creatinine and urea levels. Blood samples were analyzed for hemoglobin (Hb), red blood cell count (RBCs), total leukocyte count (TLC), hematocrit (HCT), mean corpuscular volume (MCV), mean corpuscular hemoglobin (MCH), mean corpuscular hemoglobin concentration (MCHC) and platelet count. Moreover, breast tissue histology was examined (Bhapkar *et al.*, 2025).

Statistical analysis

Mean ± standard deviation (SD) was used to express the data. Once the normality of the data was confirmed, one-way ANOVA and Dunnett's post hoc test were used for statistical analysis. Statistical analyses were performed using GraphPad Prism version 8.0 (GraphPad Software, LLC, San Diego, CA, USA) and IBM SPSS Statistics version 22.0 (IBM Corp., Armonk, NY, USA). The criteria for statistical significance were $p < 0.05$, $p < 0.01$, $p < 0.001$ and $p < 0.0001$.

RESULTS

Determination of loading capacity and encapsulation efficiency

The amount of Tamoxifen incorporated into the nanoparticles is 4.19 ± 0.32 mg (loading capacity), which equals the theoretical drug concentration within the nanoparticles. The encapsulation efficiency of Tamoxifen in the PLGA nanoparticles is 96.41 ± 0.66% and in the Gemifloxacin liposomes is 91.22 ± 1.1%.

In-vitro drug release study of Tamoxifen citrate-loaded nanoparticles and Gemifloxacin-loaded liposomes

Tamoxifen citrate-loaded PLGA nanoparticles were used for *in-vitro* drug delivery in PBS (pH 7.4) containing 1% Tween 80. Due to Tamoxifen's very low water solubility, a solubility-enhancing agent had to be added to maintain sink conditions and obtain quantifiable UV-Vis concentrations for the release tests.The first 24 hours showed an initial burst release, after which the PLGA nanoparticles containing Tamoxifen exhibited a steady drug-release pattern.The primary cause of this first stage of drug release is thought to be the drug's desorption or diffusion, which occurs at the large surface area of the nanoparticles or at sites where it is only loosely bound to the polymer matrix.

Tamoxifen and Gemifloxacin exhibited cumulative drug releases of 48.01% and 56.64%, respectively, at the end of the study. Model fitting showed that the Korsmeyer–Peppas model yielded the highest correlation coefficient (R^2 = 0.973 for Tamoxifen and R^2 = 0.883 for Gemifloxacin), indicating that it best described the release behavior. The comparatively lower cumulative release observed after 96 h indicates that a fraction of the encapsulated drug remained entrapped within the polymeric core, which is consistent with the controlled-release characteristics of PLGA-based hybrid nanoparticles reported in previous studies. It was anticipated that the remaining unreleased medication was either firmly entrapped within the nanoparticle matrix or strongly linked to PLGA molecules, primarily through matrix erosion or diffusion under sink conditions. Diffusion plays a major role in controlling the release mechanism when drug diffusion outpaces matrix disintegration (Fig. 1).

Article in Press

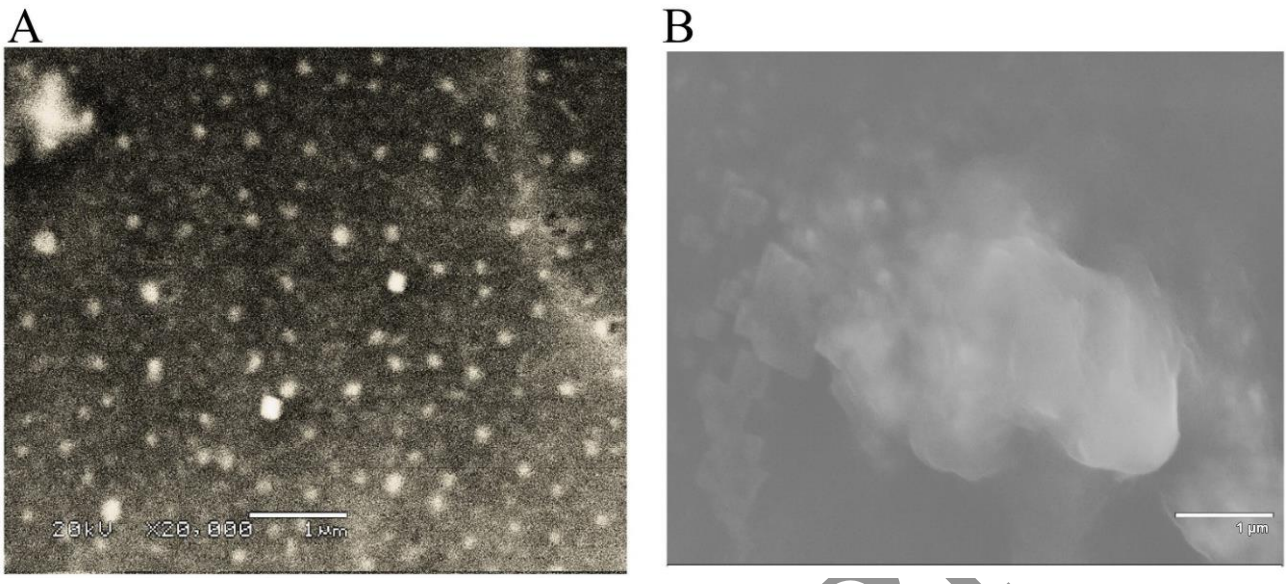


Fig. 3: SEM image of (A) Tamoxifen-loaded PLGA nanoparticles and; (B) Co-loaded hybrid nanoparticles.

Characterization

Calibration curve of tamoxifen and gemifloxacin

The calibration curve for Tamoxifen and Gemifloxacin was performed in a 7.4-pH buffer solution. Samples with different concentrations were analyzed in a UV spectrophotometer. Microsoft Excel 16 was used to plot the graph (Fig. 2).

Particle size and zeta potential

Particle size is a quantitative physical characteristic of nanocarriers and a critical factor in their characterization. The particle size, PDI and zeta potential of the three independently prepared batches are presented as mean ± standard deviation (SD) in Table 2. No statistically significant differences were observed among the batches for these parameters ($p > 0.05$), indicating good batch-to-batch reproducibility. The particle size of Tamoxifen nanoparticles, Gemifloxacin liposomes and LCHNPs was measured at 175.3 nm with a charge of 5.5 mV, 201.2 nm with a charge of -12.9 mV and 215.7 nm with a charge of 0.6 mV, respectively. A positive value of NPs is due to the presence of chitosan. So, positively charged Tamoxifen NPs are coated with negatively charged Gemifloxacin-loaded LPs.The PDI values of Tamoxifen nanoparticles, Gemifloxacin liposomes and LCHNPs were 0.03 ± 0.02, 0.25 ± 0.02 and 0.07 ± 0.03, respectively, indicating relatively narrow particle-size distributions. (Table 2).

Scanning electron microscopy

Scanning electron microscopy showed a relatively smooth surface for the Tamoxifen-loaded PLGA nanoparticles (Panel A). In comparison, the co-loaded hybrid nanoparticles displayed a distinct surface morphology after lipid–polymer fusion (Panel B). The difference in surface appearance between the two formulations is consistent with the incorporation of the lipid layer around the polymeric nanoparticle core (Fig. 3).

Fourier-transform infrared spectroscopy (FTIR)

FTIR (Fourier Transform Infrared Spectroscopy) is a basic yet very important technique for the identification of materials; more so, it helps in revealing and determining not only the molecular structure of a given substance but also the functional groups and their respective bonding strength and arrangement, for instance, in homopolymers, copolymers, polymer composites and other polymeric materials. FTIR spectra corresponding to Tamoxifen citrate are (from left to right) the ketone (C=O) at 1,737.51 cm-1, amine (N-H bend) at 1,581.36 cm-1, aromatic ring at 844.88 cm-1, phenolic C-O at 1361.05 cm-1, aliphatic alcohol at 3396.21 cm-1 and ether at 1043.78 cm-1. The FTIR spectrum of Tamoxifen nanoparticles shows slight deviations from the FTIR spectrum of Tamoxifen with the peaks from 3396.21 cm−1 to 3342.07 cm−1 allocated to the OH group, 1043.78 cm−1 to 1054.68 cm−1 to C-O stretch of ether and 1361.05 cm−1 to 1374.09 cm−1 to the phenolic C-O. The FTIR spectrum of pure powder Gemifloxacin mesylate showed peaks attributed to (C-F) bending at 1038.72 cm-1 and O–CH3 bending at 1455.03 cm-1, R–COOH stretching at 1173.91 cm-1, N–H Scissoring at 1627.63 cm-1. Aromatic–C=O Stretching at 1704.32 cm-1 and C–H Rocking at 729.69 cm-1. The FTIR spectrum of Gemifloxacin liposomes displays rather modest alterations of the peaks from 1038.72 cm-1 to 1054.70 at C-F and Aromatic–C=O Stretching from 1704.32 cm-1 to 1636.5 (Fig. 4).

Stability study

The storage stability of the lyophilized lipid-coated hybrid nanoparticles (LCHNPs) was investigated under refrigerated (4 ± 2°C) and controlled room-temperature (25 ± 2°C/60 ± 5% RH) conditions for 90 days. The physicochemical characteristics of the formulation at different storage intervals are summarized in table 3.

Article in Press

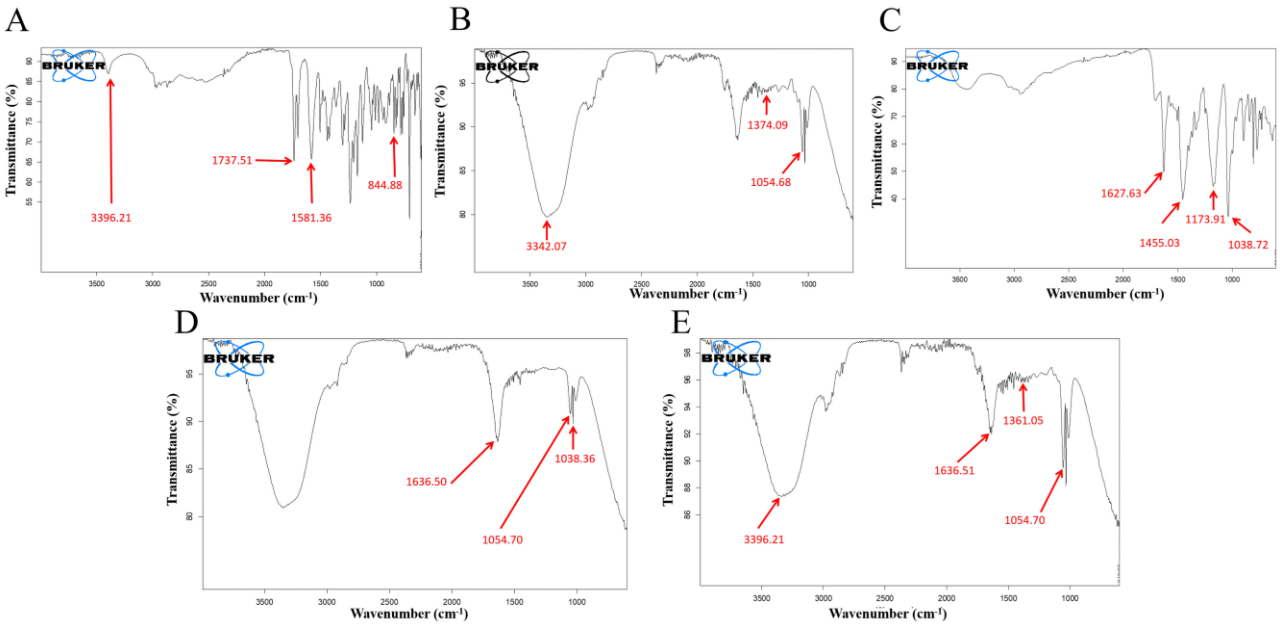


Fig. 4: FTIR spectra of (A) Tamoxifen drug; (B) Tamoxifen nanoparticles; (C) Gemifloxacin drug; (D) Gemifloxacin liposomes and; (E) LCHNPs.

Table 3: Stability evaluation of lyophilized lipid-coated hybrid nanoparticles (LCHNPs) stored under refrigerated (4 ± 2°C) and controlled room-temperature (25 ± 2°C/60 ± 5% RH) conditions for 90 days. Particle size, polydispersity index (PDI) and zeta potential were determined at predetermined intervals. Data are presented as mean ± SD (n = 3).

Storage condition	Time	Particle size (nm)	PDI	Zeta potential (mV)
4 ± 2°C	Day 0	215.7 ± 2.3	0.07 ± 0.03	+0.60 ± 0.10
	30 Days	217.1 ± 2.5	0.08 ± 0.02	+0.55 ± 0.09
	60 Days	218.5 ± 2.8	0.09 ± 0.03	+0.49 ± 0.08
	90 Days	220.3 ± 3.1	0.10 ± 0.03	+0.44 ± 0.08
25 ± 2°C / 60 ± 5% RH	Day 0	215.7 ± 2.3	0.07 ± 0.03	+0.60 ± 0.10
	30 Days	220.6 ± 3.2	0.10 ± 0.03	+0.47 ± 0.09
	60 Days	225.8 ± 3.6	0.12 ± 0.03	+0.36 ± 0.07
	90 Days	231.4 ± 4.1	0.14 ± 0.04	+0.29 ± 0.06

Throughout refrigerated storage, the formulation remained highly stable, showing only marginal variations in its physicochemical properties. The mean particle size increased slightly from 215.7 ± 2.3 nm at day 0 to 220.3 ± 3.1 nm after 90 days. Likewise, only a minimal increase in PDI was observed, indicating that the nanoparticles retained a uniform size distribution during storage. The zeta potential exhibited a small decline over time, while encapsulation efficiency and drug loading remained largely unchanged, suggesting effective retention of both Tamoxifen and Gemifloxacin within the hybrid carrier. A slightly greater degree of change was observed under room-temperature storage. After 90 days, the average particle size reached 231.4 ± 4.1 nm, accompanied by a modest increase in PDI and a gradual reduction in zeta potential. Importantly, the formulation remained readily dispersible after reconstitution, with no visible signs of aggregation, sedimentation, or phase separation under either storage condition.

Overall, the results indicate that the lyophilized LCHNPs maintained their physicochemical integrity during storage, with refrigerated storage preserving formulation characteristics better than room-temperature storage.

MTT assay

According to the data, the nanoparticle hybrid Lipid-coated showed the highest cytotoxicity against MCF-7 cells compared with the drug TMX alone. Previous studies have demonstrated that the nanoformulation of TMX is less toxic to cancer cells than the free drug. The selectivity index values were determined using the provided equation. The SI values for Gemifloxacin, Gemifloxacin liposomes, Tamoxifen, Tamoxifen nanoparticles and the co-loaded formulation were 2.01, 2.18, 3.59, 4.24 and 5.62, respectively. These values suggest that LCHNPs can produce a more potent synergistic effect than the free forms (Fig. 5; Table 4).

Article in Press

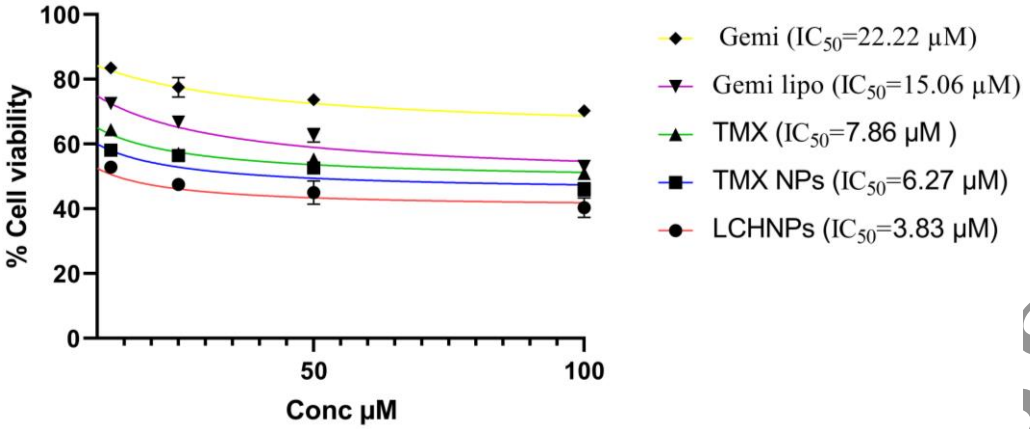


Fig. 5: Percentage viability of MCF-7 cells after exposure to Gemi, Gemi lipo, TMX, TMX NPs and LCHNPs formulation. The mean ± standard deviation from three separate experiments is shown in the data.

Table 4: IC_{50} and Selectivity index on Vero and MCF-7 cell lines.

Drugs	Cell lines	IC_{50} µM	Selectivity index	Remarks
Tamoxifen	Vero	28.25	3.59	Anticancer potential
Tamoxifen	MCF-7	7.86		
Tamoxifen nanoparticles	Vero	26.59	4.24	Significant anticancer potential
Tamoxifen nanoparticles	MCF-7	6.27		
Gemifloxacin	Vero	44.49	2.01	Anticancer potential
Gemifloxacin	MCF-7	22.22		
Gemifloxacin liposomes	Vero	32.78	2.18	Anticancer potential
Gemifloxacin liposomes	MCF-7	15.06		
Lipid-coated hybrid nanoparticles	Vero	21.51	5.62	Significant anticancer potential
Lipid-coated hybrid nanoparticles	MCF-7	3.83		

Gene expression analysis by RT-PCR

CT value of expression analysis

Fold changes in gene expression were determined from the cycle threshold (Ct) values using the Livak method. The expression levels of *CHEK2* and BRCA1 genes were quantified using Rotor-Gene Q. The expression was analyzed by adjusting the threshold value to 0.2. CT-value of *CHEK2*, *BRCA1* and reference gene (GAPDH) was obtained after the end of the reaction. For specific amplification and dissociation of cDNA, the melt curve was run during the reaction and analyzed at the end.

The mean (± SD) of the *CHEK2* gene in the treatment group was 24.44 ± 0.64 and in the control group was 26.96 ± 0.94. The mean values indicate that expression in the treatment group was upregulated compared with the control group. The mean ± SD of the *BRCA1* gene in the treatment group was 27.48 ± 0.89 and in the control group was 25.73 ± 0.25. The mean values indicate that expression in the treatment group was slightly downregulated compared with the control group.

Comparison of the expression ratio of the CHEK2 gene

The F-statistic (test statistic) of the one-way ANOVA was 4.08 and the *p*-value was 0.05, indicating that the variances of the four groups are unequal. The mean and standard deviation (mean ± SD) of control was 0.34 ± 0.29 fold change increased, in Gemifloxacin liposomes (mean ± SD) was 1.02 ± 0.29 fold change increased, in Tamoxifen nanoparticles its increased in fold change was 1.96 ± 0.42 and in Tamoxifen+Gemifloxacin co-loaded nanoparticles its increased was 2.67 ± 1.66. At the 0.05 level, the mean difference is significant. Statistical analysis shows a significant difference in *CHEK-2* gene expression levels in breast cancer between treatments and controls. CHEK2 gene expression was upregulated in female breast cancer patients (Fig. 6 a).

Comparison of expression ratio of BRCA1 gene

The test statistic (F value) of one-way ANOVA was 14.7 and the p-value was 0.01, indicating that the variances of the four groups are not equal. The mean and standard deviation (mean ± SD) of control was 2.51 ± 0.54 fold change increased, in Gemifloxacin liposomes (mean ± SD) was 1.77 ± 0.43 fold change increased, in Tamoxifen nanoparticles its increased in fold change was 0.93 ± 0.22 and in Tamoxifen + Gemifloxacin co-loaded nanoparticles its increased 0.65 ± 0.19. Statistical analysis reveals a significant difference in *BRCA1* gene expression levels between breast cancer patients treated with different therapies and those in the control group. The expression of the *BRCA1* gene was down-regulated in females with breast cancer (Fig. 6 b).

Article in Press

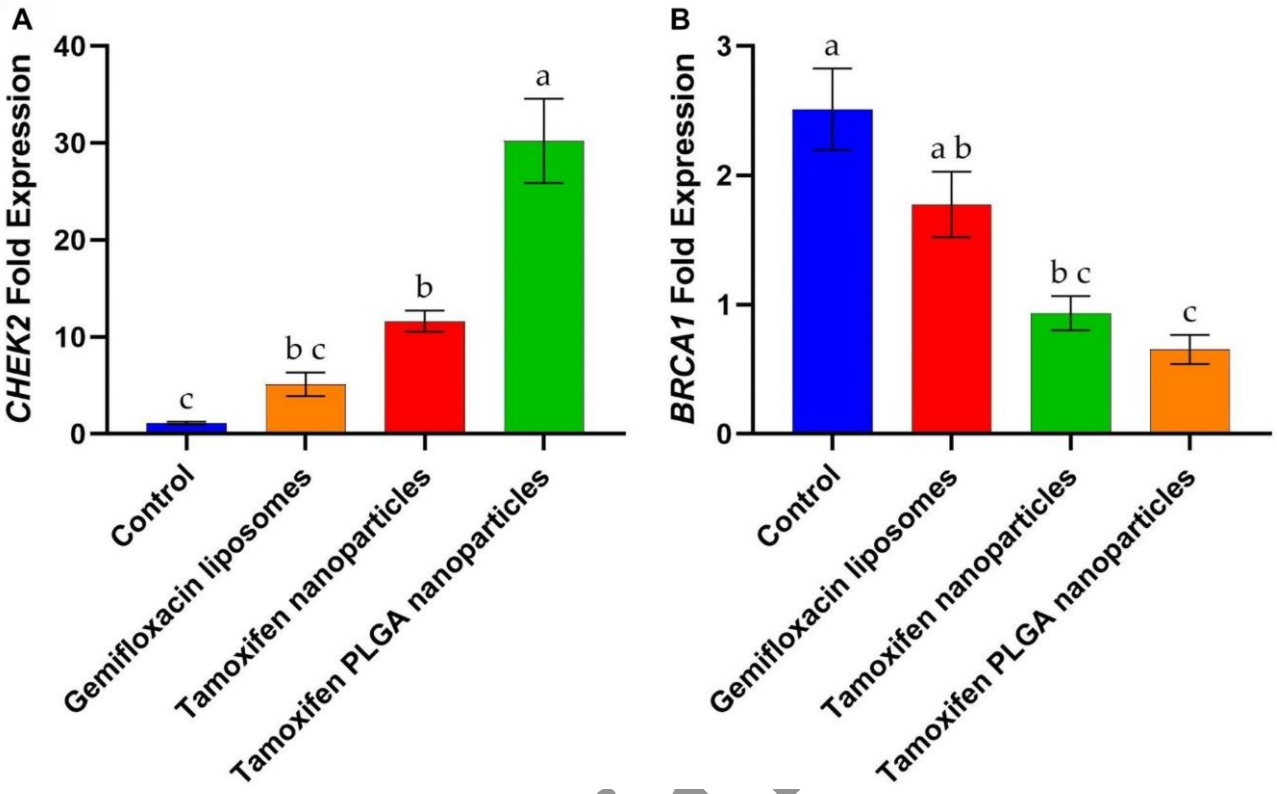


Fig. 6: Relative mRNA expression of (A) *CHEK2* and; (B) BRCA1 genes following treatment with gemifloxacin liposomes, tamoxifen nanoparticles and tamoxifen-loaded PLGA nanoparticles. Gene expression levels were quantified by quantitative real-time PCR (qRT-PCR), normalized to GAPDH as the internal reference gene and expressed as relative fold change. Data are presented as mean ± SD. Statistical significance was determined using one-way ANOVA followed by Tukey's multiple comparison test. Bars bearing different superscript letters differ significantly ($p < 0.05$), whereas bars sharing the same superscript letter are not significantly different.

In-vivo studies

Effect on tumor incidence and variation in tumor weight

After 16 weeks, the animals were dissected and found tumor nodules in every rat in the DMBA group, indicating a 100% incidence. Meanwhile, the rats in the DMBA-treated group that received free Gemifloxacin showed an 83.3% tumor incidence. As for the free Tamoxifen drug group and the Lipid-coated hybrid nanoparticles group, tumor incidence was 50% and 16.7%, respectively, as presented in Table 5.

In addition, the DMBA group of rats had the highest maximum tumor weight (16.50 ± 3.22 g) and the average tumor weight of the group with DMBA+ LCHNPs was the lowest (2.833 ± 0.752 g). Whereas the free Tamoxifen drug group and the group with free Gemifloxacin drug were found to have tumor weights of 10.11 ± 1.94 g and 12.17 ± 2.31 g, respectively (Fig. 7).

Biochemical analysis

Biochemical parameters are widely used to assess organ function and systemic responses following pharmacological interventions. In the present study, serum bilirubin levels in animals receiving the formulated treatments remained largely comparable to those of the normal control group, whereas a pronounced elevation was observed in rats exposed to DMBA alone. Liver-associated enzymes serve as sensitive markers of hepatic stress and damage to hepatocytes or biliary structures is commonly reflected by increased circulating levels of alanine aminotransferase (ALT), alkaline phosphatase (ALP) and aspartate aminotransferase (AST). A significant rise in these enzymes was recorded in the DMBA-treated group, while values in rats administered free Tamoxifen, free Gemifloxacin, or lipid-coated hybrid nanoparticles (LCHNPs) remained within physiological limits. The observed enzymatic elevation in the DMBA group may reflect inflammatory responses and increased metabolic burden associated with the detoxification of xenobiotic compounds (Dakrory *et al.*, 2015).

Evaluation of renal function revealed that serum creatinine levels were markedly increased in animals treated with DMBA compared with the normal control group, whereas the difference between the Free Gemifloxacin and normal control groups was not statistically significant. In contrast, creatinine values in the remaining treatment groups did not differ significantly from normal controls.

Article in Press

Table 5: Tumor incidence and nodule burden in experimental groups

S. No.	Groups	Number of rats with nodules/ Total number of rats	Tumor incidence (%)	Total number of nodules observed
1	Normal control	0/6	0	0
2	DMBA control	6/6	100	15
3	DMBA control + free Tamoxifen	3/6	50	7
4	DMBA control + free Gemifloxacin	5/6	83.3	11
5	DMBA control + LCHNPs	1/6	16.7	2

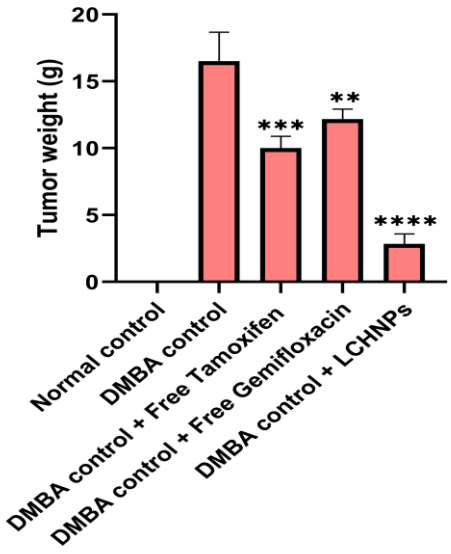


Fig. 7: Comparison of tumor weight in the treatment groups. ** indicates $p < 0.01$, *** indicates $p < 0.001$ and **** indicates $p < 0.0001$.

Similarly, urea concentrations were substantially elevated in the DMBA-treated rats, suggesting compromised renal function and possible structural alterations within renal tissues. Further assessment of total serum bilirubin confirmed that only DMBA exposure resulted in a significant increase, while no meaningful changes were detected in animals receiving nanoformulated treatments (Karimi *et al.*, 2020). When considered collectively, the biochemical findings indicate that LCHNP administration did not adversely affect hepatic or renal physiology. A summary of the biochemical parameters measured in albino rats following treatment is presented in figure 8.

Hematological analysis

The Free Tamoxifen and Free Gemifloxacin groups showed changes in platelet and total leukocyte counts, while the LCHNPs group exhibited values generally closer to those of the Normal Control group..The DMBA group, Free Tamoxifen drug and free Gemifloxacin drug showed varying changes in Hemoglobin and RBC (Red Blood Cell) count compared with the Normal Control group.. It was noted that the parameters varied only slightly in LCHNPs, which, in turn, indicated that this formulation had a safe profile. The hematological analysis results are shown in table 6.

Histopathological examination

Changes in breast tissues were observed after DMBA was administered to albino female rats; the pathogenesis of mammary carcinomas was investigated (Patil *et al.*, 2026). The breast portion from normal rats (NC) did not show any signs of cancer in the histopathology reports. Each cell was characterized by round-to-oval vesicular nuclei, with some displaying nucleoli and somewhat eosinophilic cytoplasm.Breast tissue slices from LCHNPs in rats given DMBA showed a bounded lesion with patches of fibrosis and adenosis. No indication of cancer was found. Normal ductal epithelial lining surrounding the narrowed lumen and the outer exiguous layer of myoepithelial cells were seen in the mammary glands of non-treated rats (NC). The latter had a large number of fat cells and were covered by fibrous connective tissue. DMBA-treated rats exhibited varying degrees of morphological defects across their glands, which were characteristically accompanied by one or more aberrant pattern combinations. The ducts of most glands treated with DMBA were slightly expanded and contained dispersed cell clusters. The second lesion observed in the mammary glands of the DMBA-treated rats was an increase in cell density in the terminal ducts, which was correlated with an increase in cell counts.

Article in Press

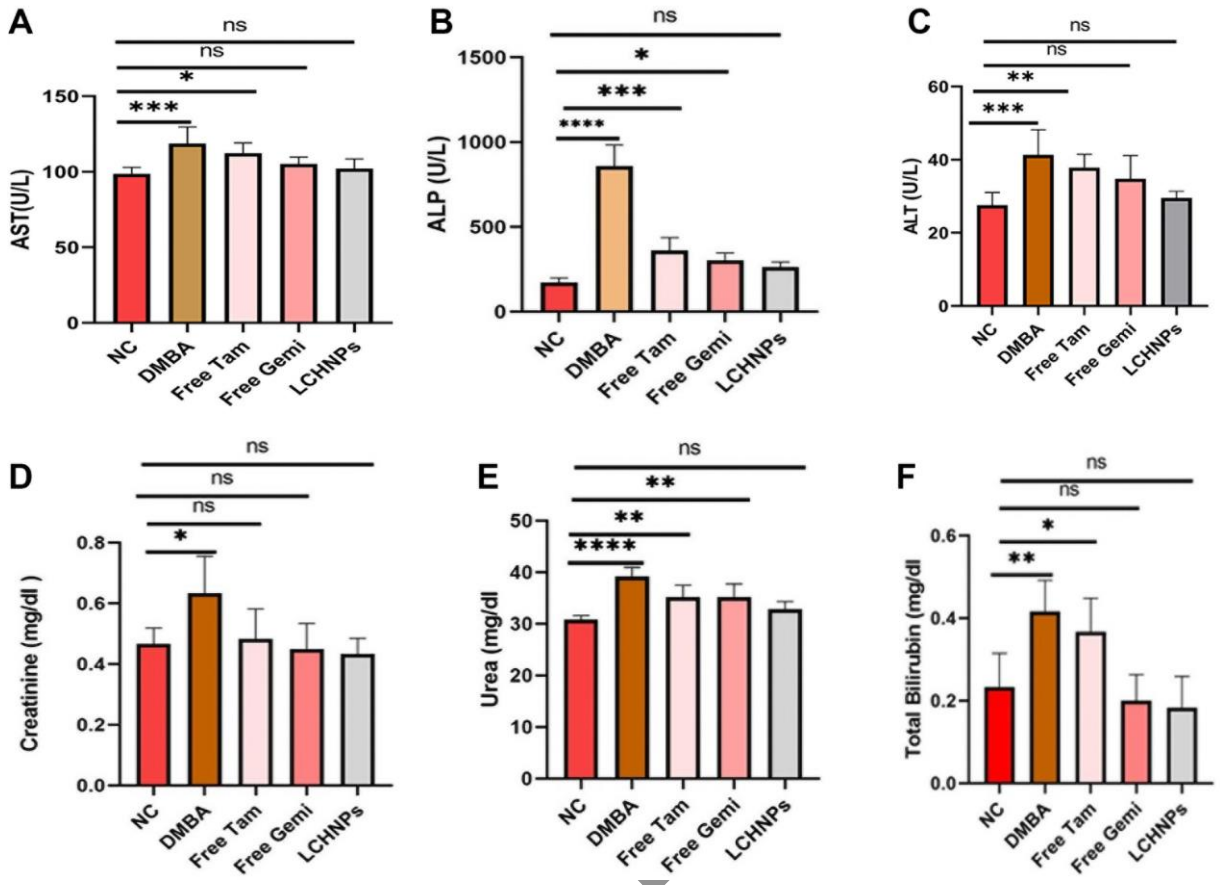


Fig. 8: Comparison of biochemical parameters including (A) AST, (B) ALP, (C) ALT, (D) Creatinine, (E) Urea and (F) Total Bilirubin of albino rat blood following treatment with the formulations. Significance levels are indicated by asterisks: * indicates $p < 0.05$, ** indicates $p < 0.01$, *** indicates $p < 0.001$, and **** indicates $p < 0.0001$.

Table 6: Comparison of hematological parameters among the experimental groups.

Sr. No.	Blood **b**iomarkers	NC (Mean ± SD)	DMBA (Mean ± SD)	Free Tam (Mean ± SD)	Free **g**emi (Mean ± SD)	LCHNPs (Mean ± SD)
1	Hb (g/dL)	13.15 ± 0.72	9.750 ± 0.36***	10.33 ± 0.68 ***	10.93±0.94***	12.60 ± 0.65*
2	RBCs (×10^6/µl)	5.58 ± 0.25	3.88 ± 0.25***	5.10 ± 0.17**	5.08 ± 0.09**	5.33 ± 0.18ns
3	TLC (x10^3/µl)	7.75 ± 0.13	3.26 ± 0.33***	4.05±0.16***	5.95 ± 0.28**	6.63 ± 0.26**
4	HCT (%)	28.10 ± 0.67	20.32 ± 0.87***	24.0± 0.60 **	25.42 ± 0.86**	26.43 ± 0.99*
5	MCV (fL)	48.42 ± 0.31	49.25 ± 0.40*	48.50±0.65ns	47.82 ± 0.90 ns	48.63 ± 0.15 ns
6	MCH (pg)	18.28 ± 0.18	17.52 ± 0.19**	17.15±0.05**	18.37 ± 0.13 ns	18.22 ± 0.09 ns
7	MCHC (g/dL)	47.52 ± 0.27	44.07 ± 0.13**	44.95±0.28**	45.42 ± 0.27*	46.75 ± 0.19*
8	Platelets (×10^3/µl)	637.0 ± 4.85	348.0 ± 9.63***	131.5±7.79***	585.3 ± 5.42**	623.3 ± 11.71*

These alterations in mammary glands were called hyperplastic. Normal breast tissue histology showed blood vessels, alveoli lined by cuboidal epithelial cells, interlobular secretory ducts, adipose cells, lactiferous ducts and dense connective tissue and note the changes among them compared with cancerous tissues. In the NC group, lobules, glands and ducts are intact, with no sign of malignancy. In the DMBA group, lobules are altered, glands and ducts are abnormal and tumor glands are present. In the Free TMX group, lobules, glands and ducts are abnormal and slightly altered. In the Free Gemifloxacin group, lobules and glands are altered; malignancy can be seen with a comedo pattern, while in LCHNPs, the Lobules, glands and ducts are intact and malignancy is not seen. Histological examination demonstrated infiltrating neoplasm composed of cells grouped into glands in tumor-induced rats receiving only DMBA treatment (Fig. 9).

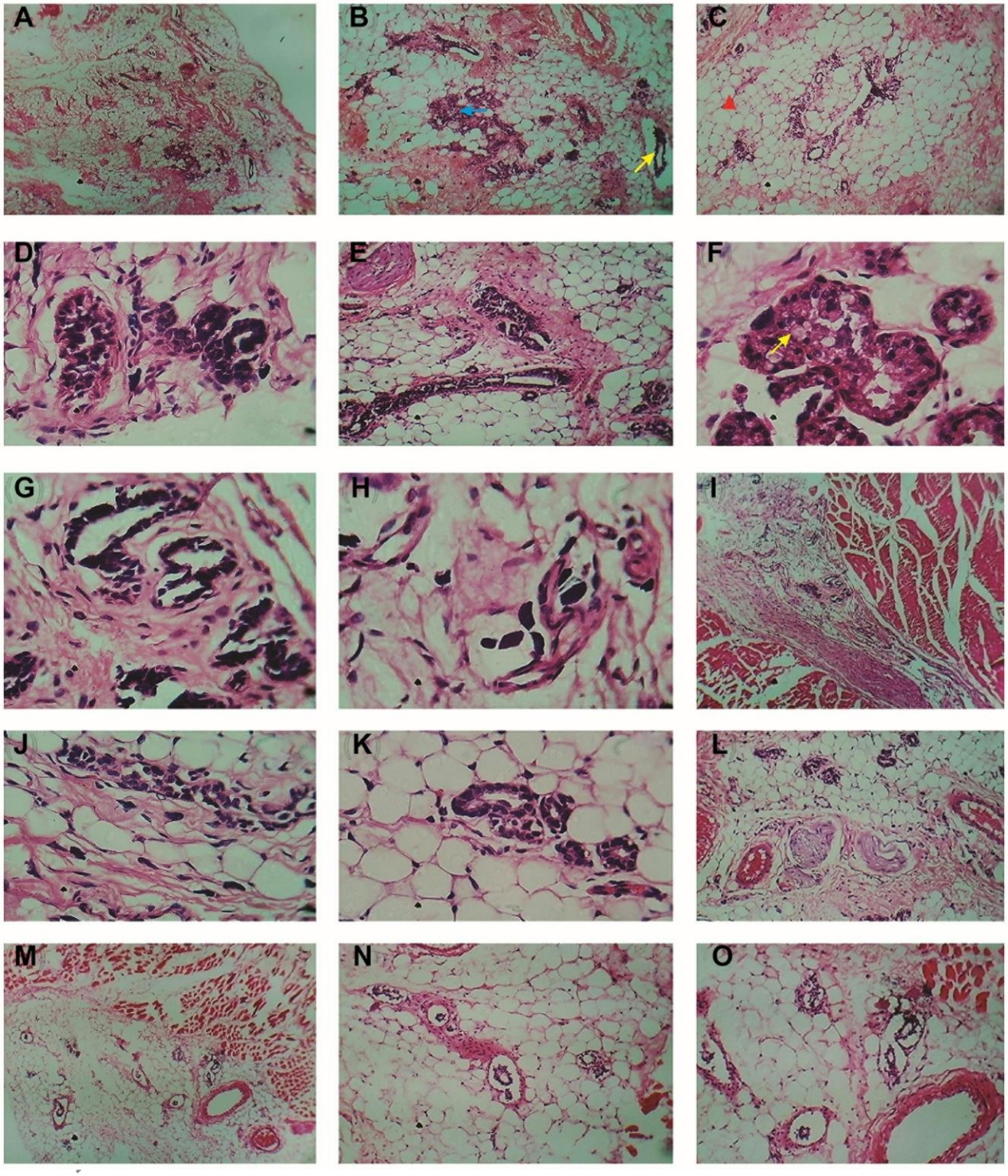


Fig. 9: Histological examination of mammary gland tissues from different experimental groups. (A–C) Normal control group showing preserved lobular structures (blue arrow) and intralobular ducts (yellow arrow); red triangle in (C) indicates a normal duct; (D–F) DMBA-treated group displaying disrupted architecture, cellular atypia and tumor embolus formation (yellow arrow in F); (G–I) Tamoxifen-treated group showing partial restoration of normal architecture and reduced atypia; (J–L) Gemifloxacin-treated group revealing moderate preservation of tissue structures with decreased neoplastic changes; (M–O) LCHNPs-treated group exhibiting marked improvement with near-normal lobular and ductal morphology and reduced pathological alterations. Magnification: 40× for panels (D), (F), (G), (H), (I), and (K); 10× for all remaining panels.

DISCUSSION

This study demonstrates the successful development of lipid-coated hybrid nanoparticles (LCHNPs) as a dual-drug delivery platform for breast cancer therapy, integrating Tamoxifen and Gemifloxacin within a single nanoplatform. By combining a PLGA-based polymeric core with a lipid shell, the formulation was designed to exploit the structural stability of polymeric nanoparticles alongside the biomimetic and drug-retentive properties of liposomes (Yao *et al.*, 2020). The collective findings from physicochemical, biological and *in-vivo* studies confirm that this hybrid design offers clear advantages over free drugs and single-drug nanoformulations. Liposome-based drug delivery systems functionalized for breast cancer treatment remain an important area of research, with recent studies highlighting their ongoing potential to improve targeted therapeutic outcomes (Bishal *et al.*, 2025).

In the current research work, PLGA nanoparticles encapsulating Tamoxifen were fabricated using a solvent evaporation technique; Gemifloxacin liposomes were prepared using the thin-film hydration technique; and lipid-polymer hybrid nanoparticles were created using the fusion method (Ain *et al.*, 2025; Patil *et al.*, 2026). Previous studies have shown that the combination of Tamoxifen and fatostatin enhances the antitumor response in estrogen receptor-positive (ER-positive) breast cancer and may improve the therapeutic profile compared with either agent alone (Liu *et al.*, 2020; Pandey *et al.*, 2015). Hormonal-dependent breast cancer and colon cancer cell lines were the subject of studies that confirmed that only Gemifloxacin among fluoroquinolones (FQs) can hinder metastasis in the case of breast cancer (Chen *et al.*, 2014; Kan *et al.*, 2013). These nanoparticles allow encapsulation of hydrophilic and hydrophobic drugs: Tamoxifen as the core and Gemifloxacin in the lipid bilayer shell. Furthermore, while the combined administration of Tamoxifen and Gemifloxacin produced improved anticancer activity compared with the individual formulations, formal pharmacological synergy was not evaluated using quantitative approaches such as Combination Index or Bliss independence analysis. Therefore, the observed effects should be interpreted as evidence of enhanced therapeutic activity rather than as confirmed drug synergy. This system may increase therapeutic efficacy, circulation time and drug bioavailability while minimizing systemic toxicity (Massadeh *et al.*, 2020). However, as pharmacokinetic and biodistribution studies were not conducted in the present work, these potential benefits remain inferential and require direct experimental confirmation.

The dimensions of the nanoparticles, liposomes and co-loaded formulation were 175.3 ± 1.97 nm, 201.2 ± 2.45 nm and 215.7 ± 2.25 nm, respectively, while the zeta potentials of the nano, lipo and co-loaded formulations were 5.5 mV, -12.9 mV and 0.6 mV, respectively. Although the zeta potential of the lipid-coated hybrid nanoparticles was close to neutral (+0.6 mV), no evidence of particle aggregation or precipitation was observed during storage. This finding suggested that colloidal stability was maintained predominantly through steric stabilization provided by the phospholipid coating rather than electrostatic repulsion alone. However, colloidal stability in lipid-coated hybrid nanoparticles is not governed exclusively by surface charge. The presence of the phospholipid shell and DSPE-PEG2000 provides effective steric stabilization by creating a hydrated polymer layer around the nanoparticle surface, thereby reducing van der Waals attraction and minimizing particle aggregation. Process of drug delivery using a combination of nanoparticles and liposomes has been reported, with release percentages of 96.41 ± 0.66% and 91.22 ± 1.1% for the respective methods. These percentages were consistent with the previously reported value (85.7%) for polymer-lipid nanoparticles (Jeong *et al.*, 2001). The FTIR spectra of Tamoxifen NPs and Gemifloxacin revealed distinct characteristic peaks consistent with previous studies (Sadeek *et al.*, 2015; Sahana *et al.*, 2010). The lipid-coated hybrid nanoparticles demonstrated satisfactory stability over a 90-day storage period under both refrigerated and room-temperature conditions. Only a minor increase in particle size was detected during storage, particularly under refrigerated conditions. Such changes were commonly observed in polymeric nanocarriers and generally associated with gradual polymer relaxation or limited particle interactions rather than irreversible aggregation. Since the increase in particle diameter was relatively small, the formulation remained within the optimal nanoscale range required for efficient passive tumor accumulation. The low PDI values recorded throughout the study indicated that the particle population remained homogeneous during storage. Likewise, the slight reduction in zeta potential over time did not appear to compromise colloidal stability, as no visible aggregation or precipitation was observed after reconstitution. Although the developed lipid-coated hybrid nanoparticles exhibited satisfactory physicochemical stability during storage, their stability in physiological environments containing serum proteins was not evaluated in the present study.

The present study was performed using the MCF-7 breast cancer cell line as an initial proof-of-concept model. Although this model is widely used to evaluate Tamoxifen-based therapies, additional investigations using multidrug-resistant, HER2-positive and triple-negative breast cancer cell lines are necessary to determine the broader therapeutic applicability of the developed lipid-coated hybrid nanoparticles. The cytotoxicity assay revealed that TNPs induced greater cell death compared to free Tamoxifen citrate (Sandoval-Vasquez *et al.*, 2026). The cytotoxicity of the latter was concentration-dependent and cell viability was significantly reduced from 70.13% to

Article in Press

21.81% when the concentration was increased from 12.5 µM to 200 µM (Maji *et al.*, 2014). This improvement can be attributed to the combined therapeutic effect of Tamoxifen-mediated estrogen receptor blockade and Gemifloxacin-induced DNA damage, which collectively drive cancer cells toward apoptotic pathways.

The gene *CHEK2*, which is responsible for DNA repair and cell-cycle regulation, was reported to be up-regulated in the LCHNP-treated group with a remarkable fold change of 1.96, while BRCA1 was down-regulated by 0.93 in the LCHNP treated group. The observed upregulation of *CHEK2* and downregulation of *BRCA1* suggested that the developed formulation may influence molecular pathways associated with the cellular DNA damage response. However, these findings are based exclusively on transcript-level data and require validation through complementary protein expression analyses and functional assays to confirm their biological significance.

This coordinated modulation may indicate a synthetic vulnerability-like effect, whereby breast cancer cells become less capable of coping with accumulated genomic damage, thereby increasing their sensitivity to treatment. However, this interpretation remains hypothetical because functional assays evaluating DNA damage, apoptotic signaling and protein expression were not included in the present study. Further mechanistic investigations are therefore required to validate this proposed mode of action. These results were also consistent with a previous investigation that indicated a significant change in the gene expression of cancer cells in the LCHNPs-treated group (Hoxha *et al.*, 2024; Kliesch *et al.*, 2022).

The outcome of the current *in-vivo* experiment indicated a significant reduction in both tumor incidence and weight in the LCHNP-treated group. More specifically, tumor occurrence was only 16.7% in the LCHNP-treated group, whereas it was 100 percent in the DMBA control group. Moreover, the mean tumor weight in the LCHNP-treated group was significantly lower (2.83 g) than that of the DMBA-treated alone group (16.5 g). Notably, these outcomes corroborated previous investigations showing that lipid-derived nanoparticles have enhanced stability and drug-delivery capacity in the treatment of aggressive cancer subtypes, such as TNBC. Similarly, a recent study employed nanoparticle-based chemoprevention in the DMBA-induced mammary tumor model reported comparable reductions in both tumor incidence and tumor burden (Alamelu *et al.*, 2026).

Although the developed lipid-coated hybrid nanoparticles demonstrated promising therapeutic efficacy and favorable short-term safety in the DMBA-induced breast cancer model, several limitations should be acknowledged, including the evaluation of drug release only at physiological pH (7.4), without assessment under the acidic tumor microenvironment (pH 5.0–6.5), where altered pH conditions may influence drug release and availability.Additional analytical validation, including fusion efficiency determination, analytical recovery studies and amplification efficiency assessment, is also warranted.These would further strengthen the reproducibility and robustness of the methodology and should be considered for future investigations. Furthermore, the proposed molecular mechanism was investigated only at the transcript level using *CHEK2* and *BRCA1* expression, with no protein validation (Western blot, ELISA, immunohistochemistry) performed and no apoptosis markers were measured. In addition, the limited number of biological replicates for RT-PCR reduced the statistical power of the analysis. Therefore, the present findings should be considered preliminary molecular evidence that supports the proposed mechanism of action. Another suggestion for future work is longitudinal body weight monitoring and additional formulation control groups. The biological evaluation was also restricted to a single estrogen receptor-positive MCF-7 cell line; the absence of multidrug-resistant, HER2-positive and triple-negative breast cancer models limits the generalizability of the observed antitumor effects across the molecular subtypes of breast cancer and should be addressed in future studies. Finally, pharmacokinetic, biodistribution, immunogenicity and long-term toxicity studies remain necessary before the developed formulation can be considered for clinical translation.

CONCLUSION

The lipid-coated hybrid nanoparticles developed in this study showed favorable physicochemical characteristics, controlled drug release and promising antitumor activity in the experimental breast cancer model. The dual-drug formulation containing Tamoxifen and Gemifloxacin demonstrated greater anticancer activity than the individual formulations, indicating the potential of Gemifloxacin as a repurposed adjunct to Tamoxifen. Changes in CHEK2 and BRCA1 expression may indicate involvement of DNA damage response pathways; however, these findings are limited to transcript-level analysis and require further mechanistic validation.

Acknowledgements
The authors express sincere gratitude to all who contributed to the completion of this research.

Authors' contributions
Tehreem Arshad: Writing original draft preparation, methodology and experimental performance; Muhammad Ovais Omer: Supervision, conceptualization, reviewing and final approval for the submission; Ali Sharif: Investigation, software validation and data analysis; Adeel Sattar: reviewing & editing; Arfan Ahmad: Assisted in *in-vitro* performance; Imran Tariq: Conceptualization,

Article in Press

methodology and visualization; Sajid Ali: conceptualization and methodology.

Funding
This study did not receive any external funding.

Data availability statement
The datasets generated during and/or analysed during the current study are available from the corresponding author on reasonable request.

Ethical approval
All experiments were conducted in accordance with established procedures approved by the Bioethical Committee of the University of Veterinary and Animal Sciences, Lahore, Pakistan (No. DR/183-1, dated 19-04-2023). The manuscript was prepared in accordance with the ARRIVE 2.0 (Animal Research: Reporting of *In Vivo* Experiments) guidelines. This study was performed in adherence with the ARRIVE guidelines. See supplementary file for the ARRIVE checklist.

Conflict of interest
The authors declare no conflict of interest.

REFERENCES

Adefisan-Adeoye AO, Ayanbanjo OO, Adeoye TD, Jayesimi TE, Unuofin JO, Lebelo SL and Adaramoye OA (2025). Bisdemethoxycurcumin chemoprevents 7,12-dimethylbenz(a)anthracene-induced mammary toxicity via modulation of oxidative processes. *Sci. Rep.*, **15**(1): 9170.

Agardan NBM, Degim Z, Yilmaz S, Altintas L and Topal T (2020). Tamoxifen/raloxifene loaded liposomes for oral treatment of breast cancer. *J. Drug Deliv. Sci. Technol.*, **57**: 101612.

Ain QU, Rasheed MA, Tariq I, Omer MO and Zahoor MY (2025). Development and *in-vitro* evaluation of tamoxifen and doxycycline loaded lipid-polymer hybrid nanoparticles for anticancer therapy. *Asian J. Agri. Biol.*, **13**(3): 2024256.

Al-Otaibi W (2021). Rosemary oil nano-emulsion potentiates the apoptotic effect of mitomycin C on cancer cells *in-vitro*. *Pharmacia*, **68**(1): 201-209.

Alamelu S, Venkatesan KB, Shagirtha K, Srinivasan MK and Pachaiappan P (2026). Chemopreventive potential of brucine-gold nanoparticles (BRU-AuNPs) in DMBA-induced mammary cancer via modulation of PI3K/AKT/mTOR pathway. *Appl. Biochem. Biotechnol.*, **198**(6): 4161-4187.

Alawi M, Hilles AR, Kumar M, Ansari MD and Mahmood S (2025). Lipid-polymer hybrid nanoparticles: A cutting-edge frontier in breast cancer treatment strategies. *Nanomedicine*, **20**(14): 1775-1798.

Ali S (2019). Novel lipoparticles for the synergistic chemo-photodynamic therapy of cancer cells. *PhD Thesis. Department of Pharmacy. Philipps University Marburg, Marburg, Germany.*

Ali S, Amin MU, Tariq I, Sohail MF, Ali MY, Preis E, Ambreen G, Pinnapireddy SR, Jedelska J, Schafer J and Bakowsky U (2021). Lipoparticles for synergistic chemo-photodynamic therapy to ovarian carcinoma cells: *In-vitro* and *in-vivo* assessments. *Int. J. Nanomed.*, **16**: 951-976.

Anand A, Lee KK, Chapman AR, Ferry AV, Adamson PD, Strachan FE, Berry C, Findlay I, Cruikshank A, Reid A, Collinson PO, Apple FS, McAllister DA, Maguire D, Fox KAA, Newby DE, Tuck C, Harkess R, Keerie C, Weir CJ, Parker RA, Gray A, Shah ASV, Mills NL, Alexander B, Amoils S, Armstrong R, Bularga A, Croal BL, Doudesis D, Fischbacher CM, Ford I, Fujisawa T, Harkess R, Kimenai DM, Leslie SJ, Linksted P, Lowry MTH, MacDonald C, Marshall L, Mendusic F, Norrie J, Sadat I, Stables CL, Stevens J, Stewart SD, Stirling L, Taggart C, Wereski R and Young S (2021). High-sensitivity cardiac troponin on presentation to rule out myocardial infarction: A stepped-wedge cluster randomized controlled trial. *Circulation*, **143**(23): 2214-2224.

Aziz M, Fatima R and Assaly R (2020). Elevated interleukin-6 and severe COVID-19: A meta-analysis. *J. Med. Virol.*, **92**(11): 2283-2285.

Bhapkar T, Sawarkar A, Patil M, Somkuwar A, Kaore M and Umap S (2025). Potential of neolamarckia cadamba in modulating cancer-associated anemia and biochemical imbalances in mammary tumor rats. *Int. J. Adv. Biochem. Res.*, **9**(4S): 285-289.

Bishal A, Paul P, Bera S, Patra D, Bandyopadhyay B, Debnath B and Ali KA (2025). Targeted drug delivery for breast cancer using functionalized liposomes: Preparation methods, challenges and clinical translation. *AAPS PharmSciTech*, **26**(7): 207.

Bray F, Laversanne M, Sung H, Ferlay J, Siegel RL, Soerjomataram I and Jemal A (2024). Global cancer statistics 2022: GLOBOCAN estimates of incidence and mortality worldwide for 36 cancers in 185 countries. *CA Cancer J. Clin.*, **74**(3): 229-263.

Chatterjee P and Kumar S (2022). Current developments in nanotechnology for cancer treatment. *Mater. Today Proc.*, **48**: 1754-1758.

Chen T-C, Hsu Y-L, Tsai Y-C, Chang Y-W, Kuo P-L and Chen Y-H (2014). Gemifloxacin inhibits migration and invasion and induces mesenchymal–Epithelial transition in human breast adenocarcinoma cells. *J. Mol. Med.*, **92**(1): 53-64.

da Silva JR, de Souza JB, de Oliveira LL, de Almeida Campos LA and Cavalcanti IMF (2026). Repositioning of fluoroquinolones: A new approach in antitumor therapy. *Biology*, **15**(9): 717.

Dakrory AI, Fahmy SR, Soliman AM, Mohamed AS and Amer SAM (2015). Protective and curative effects of the sea cucumber (Holothuria atra) extract against DMBA-

Article in Press

induced hepatorenal diseases in rats. *BioMed Res. Int.*, **2015**(1): 1-11.

Derismahafi Z, Farhud D, Razavirad A, Muhammadnejad A, Jahanbin B, Farivar S and Shirkoohi R (2025). NRF2 expression level and estrogen function in BRCA1-mutated breast cancer. *BMC Cancer*, **25**(1): 1622.

Firuzabadi FD and Asadi Z (2021). Experimental and computational studies of the interaction of gemifloxacin and manganese (II) gemifloxacin complex with DNA. *J. Mol. Struct.*, **1224**: 129248.

Gatto MS and Najahi-Missaoui W (2023). Lyophilization of nanoparticles, does it really work? Overview of the current status and challenges. *Int. J. Mol. Sci.*, **24**(18): 14041.

Hoxha I, Sadiku F, Hoxha L, Nasim M, Christine Buteau MA, Grezda K and Chamberlin MD (2024). Breast cancer and lifestyle factors. *Hematol. Oncol. Clin. North Am.*, **38**(1): 137-170.

Jacob S, Varkey NR, Boddu SHS, Gorain B, Rao R and Nair AB (2025). Advances in lipid-polymer hybrid nanoparticles: Design strategies, functionalization, oncological and non-oncological clinical prospects. *Pharmaceuticals*, **18**(12): 1772.

Jeong YI, Cho CS, Kim SH, Ko KS, Kim SI, Shim YH and Nah JW (2001). Preparation of poly(DL-lactide-co-glycolide) nanoparticles without surfactant. *J. Appl. Polym. Sci.*, **80**(12): 2228-2236.

Jeromin S, Eder C, Haferlach C, Haferlach T and Kern W (2019). Impact of assay procedures on detection of MR4.5 status in chronic myeloid leukemia: Optimization of cDNA synthesis. *Int. J. Lab. Hematol.*, **41**(5): e109-e112.

Kan JY, Hsu YL, Chen YH, Chen TC, Wang JY and Kuo PL (2013). Gemifloxacin, a fluoroquinolone antimicrobial drug, inhibits migration and invasion of human colon cancer cells. *BioMed Res. Int.*, 159786.

Karimi S, Arabi A, Shahraki T and Safi S (2020). Detection of severe acute respiratory syndrome Coronavirus-2 in the tears of patients with Coronavirus disease 2019. *Eye*, **34**(7): 1220-1223.

Kassab AE, Gomaa RM and Gedawy EM (2024). Drug repurposing of fluoroquinolones as anticancer agents in 2023. *RSC Adv.*, **14**(50): 37114-37130.

Kesharwani P, Kumar V, Goh KW, Gupta G, Alsayari A, Wahab S and Sahebkar A (2025). PEGylated PLGA nanoparticles: Unlocking advanced strategies for cancer therapy. *Mol. Cancer*, **24**(1): 205.

Kliesch L, Delandre S, Gabelmann A, Koch M, Schulze K, Guzman CA, Loretz B and Lehr CM (2022). Lipid–polymer hybrid nanoparticles for mRNA delivery to dendritic cells: Impact of lipid composition on performance in different media. *Pharmaceutics*, **14**(12): 2675.

Liu Y, Zhang N, Zhang H, Wang L, Duan Y, Wang X, Chen T, Liang Y, Li Y, Song X, Li C, Han D, Chen B, Zhao W and Yang Q (2020). Fatostatin in combination with tamoxifen induces synergistic inhibition in ER-positive breast cancer. *Drug Des. Devel. Ther.*, **14**: 3535-3545.

Ma T, Geng X, Shi W, Yu C, Wu X, Cui N, Zhao Z, Li H, Zhao C, Ni Q, Zhu X and Xia P (2025). γ-Oryzanol-Loaded PLGA nanoparticles: Enhanced drug delivery and therapeutic efficacy for breast cancer therapy. *Front. Bioeng. Biotechnol.*, **13**: 1675338.

Maji R, Dey NS, Satapathy BS, Mukherjee B and Mondal S (2014). Preparation and characterization of Tamoxifen citrate loaded nanoparticles for breast cancer therapy. *Int. J. Nanomed.*, **9**: 3107-3118.

Mangu K, Gandhi AN and Rizwanullah M (2026). Progress in nanotechnology-based strategies to enhance tamoxifen therapy for breast cancer management. *Pathol. Res. Pract.*, **277**: 156308.

Maretti E, Molinari S, Partel S, Recchia B, Rustichelli C and Leo E (2025). Investigating hybrid PLGA-lipid nanoparticles as an innovative delivery tool for palmitoylethanolamide to muscle cells. *Pharmaceutics*, **17**(11): 1412.

Massadeh S, Omer ME, Alterawi A, Ali R, Alanazi FH, Almutairi F, Almotairi W, Alobaidi FF, Alhelal K, Almutairi MS, Almalik A, Obaidat AA, Alaamery M and Yassin AE (2020). Optimized polyethylene glycolylated polymer–lipid hybrid nanoparticles as a potential breast cancer treatment. *Pharmaceutics*, **12**(7): 666.

Mulè C, Caputo TM, Montefusco A, Romanelli AM, Caputo I, Paolella G, Aliberti A and Cusano A (2025). PLGA nanoparticles for capsaicin delivery: Enhanced encapsulation efficiency and pro-apoptotic activity in HEPG2 cells. *Front. Bioeng. Biotechnol.*, **13**: 1617022.

Nandi U, Onyesom I and Douroumis D (2021). An *in-vitro* evaluation of antitumor activity of sirolimus-encapsulated liposomes in breast cancer cells. *J. Pharm. Pharmacol.*, **73**(3): 300-309.

Narwade M, Haldar N, Samanta R, Pawar A, Gajbhiye V and Gajbhiye KR (2025). αvβ3 integrin aptamer functionalized pH-responsive lipid polymer hybrid nanoparticles for targeted co-delivery of paclitaxel and tamoxifen. *Int. J. Biol. Macromol.*, **306**: 141754.

Pandey P, Arya DK, Kumar A, Kaushik A, Mishra YK and Rajinikanth PS (2025). Dual ligand functionalized pH-sensitive liposomes for metastatic breast cancer treatment: *In-vitro* and *in-vivo* assessment. *J. Mater. Chem. B.*, **13**(8): 2682-2694.

Pandey SK, Ghosh S, Maiti P and Haldar C (2015). Therapeutic efficacy and toxicity of tamoxifen loaded PLA nanoparticles for breast cancer. *Int. J. Biol. Macromol.*, **72**: 309-319.

Patil D, Vaishali, Randhave NV, Setia A, Kumar V, Rani K, Verma N, Agrawal N and Muthu MS (2026). Tamoxifen-loaded TPGS-PLGA nanoplatform for breast cancer therapy: Insights into drug delivery, distribution, treatment efficacy and ultrasound/photoacoustic imaging. *Nanomedicine*, **21**(5): 1-12.

Rivera MD, Vazquez-Duhalt R, Castro-Longoria E and Juarez-Moreno K (2024). Synergistic anticancer effects

Article in Press

and reduced genotoxicity of silver nanoparticles and tamoxifen in breast cancer cells. *J. Biochem. Mol. Toxicol.*, **38**(10): e23823.

Sadeek SA, Abd El-Hamid SM and El-Shwiniy WH (2015). Synthesis, spectroscopic characterization, thermal stability and biological studies of mixed ligand complexes of gemifloxacin drug and 2,2'-bipyridine with some transition metals. *Res. Chem. Intermed.*, **42**(4): 3183-3208.

Sahana B, Santra K, Basu S and Mukherjee B (2010). Development of biodegradable polymer based tamoxifen citrate loaded nanoparticles and effect of some manufacturing process parameters on them: A physicochemical and *in-vitro* evaluation. *Int. J. Nanomed.*, **5**: 621-630.

Sahin S, Kaya-Tilki E, Baysal M and Ozturk AA (2025). Preparation and evaluation of temozolomide loaded PLGA nanoparticles for the treatment of glioblastoma multiforme. *Sci. Rep.*, **15**(1): 36194.

Salimi S, Motalleb G, Dehghani H, Rahdar A, Dastjerdi K, Velasco B and Taboada P (2025). Anticancer effect of tamoxifen and Fe3O4@ SiO2@ Cu hybrid NPs on malignant human breast cancer cell (MCF-7). *J. Mol. Liq.*, **429**: 127570.

Sandoval-Vasquez C, Carcamo I, Lagos P, Munoz A, Zavala F, Colil V, Villagran-Silva F, Vasquez-Carrasco E, Hernandez-Martinez J, Valdes-Badilla P, Torrens F, Fincheira P and Sepulveda P (2026). Effectiveness of drug-loaded poly(ethylene glycol) and poly(lactic-co-glycolic-acid) nanoparticles in the *in-vitro* treatment of breast cancer: A systematic review. *Front. Pharmacol.*, **16**: 1710176.

Sharmin M and Bhuiyan AH (2019). Modifications in structure, surface morphology, optical and electrical properties of ZnO thin films with low boron doping. *J. Mater. Sci.: Mater. Electron.*, **30**(5): 4867-4879.

Uniyal P, Das Pramanik S, Pandey S, Shukla P, Roy P, Parashar D, Gupta S, Rawat R, Gaurav A and Lee VS (2026). Synergistic combinatorial anticancer potential of tamoxifen with naringin and diosmetin in MCF-7 breast cancer cells and their liposomal delivery. *Sci. Rep.*, **16**: 7646.

Wang X, Li J, Zhang W, Li P, Zhang W, Wang H and Tang B (2022). Evaluating diabetic ketoacidosis via a MOF sensor for fluorescence imaging of phosphate and pH. *Chem. Commun.*, **58**(18): 3023-3026.

Wang Y, Cheng W, Zhu J, He L, Ren W, Bao D and Piao J-G (2024). Programmed Co-delivery of tamoxifen and docetaxel using lipid-coated mesoporous silica nanoparticles for overcoming CYP3A4-mediated resistance in triple-negative breast cancer treatment. *Biomed. Pharmacother.*, **170**: 116084.

Yao Y, Zhou Y, Liu L, Xu Y, Chen Q, Wang Y, Wu S, Deng Y, Zhang J and Shao A (2020). Nanoparticle-based drug delivery in cancer therapy and its role in overcoming drug resistance. *Front. Mol. Biosci.*, **7**: 193.

Zhang W, Wang X, Li P, Zhang W, Wang H and Tang B (2020). Evaluating hyperthyroidism-induced liver injury based on in situ fluorescence imaging of glutathione and phosphate via nano-MOFs sensor. *Anal. Chem.*, **92**(13): 8952-8958.

Zhang Z, Tantai M, Ma H, Yu S, Zhang Y, Song J, Liu F, Feng G and Lu Z (2025). Synthesis and performance optimization of multi-bioactive compound-loaded nanocarriers for antimicrobial applications. *Sci. Rep.*, **15**(1): 41324.

Article in Press